

Energy-dependent Huang-Rhys factor of free excitons

Hui Zhao and H. Kalt

Institut für Angewandte Physik, Universität Karlsruhe, D-76128 Karlsruhe, Germany

(Received 9 April 2003; revised manuscript received 2 July 2003; published 11 September 2003)

We use quantum wells of the polar semiconductor ZnSe as a model system to demonstrate an energy dependence of the excitonic Huang-Rhys factor. Both the spectral shape of phonon-sideband emission and the intensity ratios of hot-exciton luminescence peaks yield identical results. We find that the Huang-Rhys factor decreases rapidly from 0.31 for cold excitons to less than 0.10 for hot excitons with a kinetic energy of about 15 meV, which is consistent with theoretical predictions. This behavior of the Huang-Rhys factor is confirmed to be independent of experimental conditions such as sample temperature and excitation wavelength. Previous (energetically integrating) experiments yielding such dependencies can be interpreted in terms of the influence of the exciton distribution.

DOI: 10.1103/PhysRevB.68.125309

PACS number(s): 78.55.-m, 78.67.De, 71.35.Cc, 63.20.Ls

Optical properties of most semiconductors near the band gap are dominated by excitonic effects. Optical spectroscopy, being the most important method in studying the excitonic properties, exploits the coupling between the photon and the exciton. Direct exciton-photon coupling without phonon participation leads to the appearance of a zero-phonon line (ZPL) in photoluminescence (PL) or absorption spectra. Phonon-assisted emission or absorption of photons by excitons introduce several satellites beside the ZPL. In polar materials, the most dominant phonon-assisted process is achieved by longitudinal-optical (LO) phonons. The resulting phonon sideband (PSB) has been widely used to study the properties of a number of important semiconductor structures.

Generally, the intensity of the n th order PSB, I_n , is related to that of ZPL, I_0 , by

$$I_n = \frac{S^n}{n!} I_0. \quad (1)$$

Here n is the number of LO phonons involved. S is called Huang-Rhys factor¹ and defined as

$$S = \sum_q \frac{|V(q)|^2}{E_{LO}}, \quad (2)$$

where E_{LO} is the LO-phonon energy (for a recent review, see Ref. 2). $V(q)$ is the matrix element for exciton-phonon interaction, with q being the wave vector involved. This matrix element, thus S , is determined by the ionic property of the lattice and the spatial distribution of the exciton wave function. For the excitons bound by lattice defects or impurities as well as that strongly confined in quantum dots, the distribution of wave function is well related to the confinement potential. Thus, S provides a quantitative description of exciton-phonon coupling property of these localizing states. By studying the Huang-Rhys factor, extensive information on properties of a large number of localizing centers in semiconductors has been obtained.³⁻²¹ However, in a typical PL experiment, one detects a large number of centers with different detailed structures and surroundings. Thus, the measured S is actually the averaged value of an ensemble com-

posed of slightly different centers. A recent experiment based on single-center detection achieves measurement of the microscopic Huang-Rhys factor of individual centers and, indeed, reveals the strong variation of S from center to center.²²

In contrast to localized excitons, a free exciton can migrate in the crystal. The S of the free exciton thus describes the intrinsic property of the crystal itself, since the spatial distribution of the wave function is no longer dominated by any particular local potential environment. By studying the PSB, S of free excitons has been investigated in several experiments²³⁻³¹ and one calculation.³² Although valuable information has been deduced from these investigations, a similar problem as in the studies of bound excitons exists: A free exciton has a center-of-mass kinetic energy, which influences the spatial distribution of wave function and thus S . The PSB originates from the recombination of excitons with different kinetic energies. Since the spectrally integrated intensities of the PSB were used in these investigations, the deduced S is again an averaged value of an ensemble composed of excitons with different kinetic energies. Since the kinetic energy distribution of excitons is sensitive to a number of experimental conditions, such an average effect may lead to controversies, as summarized in Ref. 2.

In this article, we investigate the energy-dependent Huang-Rhys factor of free excitons. By quasiresonant excitation with a low density, we create well-defined nonthermal distributions of hot excitons in ZnSe quantum wells. The intensity and spectral shape of the PSB enable us to obtain the energy-dependent Huang-Rhys factor, $S(E_k)$, with E_k being the kinetic energy of the exciton. The additional dimension of energy provides us a deeper insight into this factor. We find that the factor decreases rapidly with increasing E_k . The experimental results are well consistent with theoretical predictions. We show experimentally that the $S(E_k)$ is independent of sample temperature and excitation excess energy, E_{excess} . We also confirm with the same set of data that the S measured by using the *integrated* PSB intensity shows strong artificial dependencies on temperature and E_{excess} . These effects originate simply from the change of exciton distribution, thus the weight of the integration, by experimental conditions.

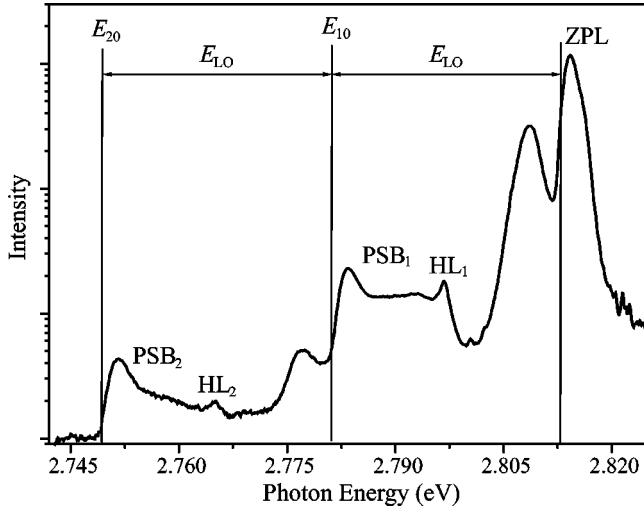


FIG. 1. Photoluminescence spectrum measured at a sample temperature of 7 K. The photon energy of the excitation laser is 2.8604 eV. This excitation condition corresponds to an excess energy of 45.9 meV and an exciton kinetic energy of 14.1 meV.

The sample studied is a 140-period ZnSe/ZnS_{0.1}Se_{0.9} multiple quantum well with a well width of 7.3 nm and a barrier width of 10.7 nm, grown by metal-organic vapor phase epitaxy. The excitation source is a cw Ti:sapphire laser pumped by an Ar-ion laser and frequency-doubled by using a beta barium borate crystal. The excitation intensity used for all measurements is below 1 kW/cm² to exclude the influence of the carrier-carrier interactions. The sample is put into a helium-flow cryostat for low-temperature measurements. The PL is dispersed by a double-grating spectrometer with a 0.75-m focal length and recorded by a cooled charged-coupled device (CCD) camera. The overall spectral resolution is about 50 μ eV.

The excitonic dynamics in this kind of polar semiconductor structure have been well understood through previous experiments.^{33–36} The laser photon with suitable energy couples to electron-hole pair states in the excitonic continuum. Then an exciton is formed through efficient LO-phonon emission. Since this exciton formation process is as fast as 100 fs, we can generate monochromatic and hot excitons with a kinetic energy $E_k = E_{\text{excess}} - E_{\text{LO}}$. In the present experiment, we can choose the value of E_k in the range of 2 to 20 meV by tuning the excitation laser wavelength. The relaxation of the hot excitons is achieved by acoustic-phonon emission and continues over several hundred picoseconds.³³ The fast-formation/slow-relaxation feature enables us to generate a well-defined, tunable, and non-thermal distribution of hot excitons under cw excitation at low temperatures, which is of crucial importance for measuring $S(E_k)$.

Figure 1 shows a PL spectrum measured at a sample temperature of 7 K. The ZPL of exciton is observed at 2.8145 eV. The peak at the low-energy side of ZPL is attributed to the direct recombination of charged excitons. The first and second order PSB's introduced by LO-phonon participation are clearly visible on the low-energy part of the spectrum (PSB₁ and PSB₂). A sharp peak (HL₁ and HL₂) is observed

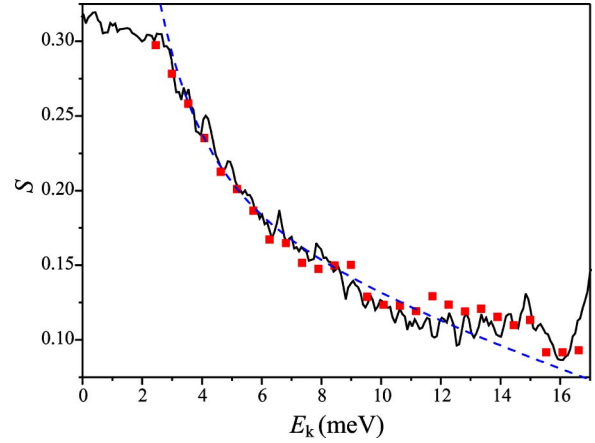


FIG. 2. (Color online) Huang-Rhys factor S as function of exciton kinetic energy. Solid curve: measured by using the ratio between the two PSB's. Squares: measured by using the HL peaks. Dashed line: calculated by using Eq. (4).

at the high-energy limit of each PSB. It is located at twice and three times E_{LO} (31.8 meV, measured by Raman spectroscopy) below the laser-photon energy, respectively. According to the above analysis, it originates from the first or second order LO-phonon-assisted recombination process of excitons right after the formation and before the first step of relaxation. We adopt the generally accepted notation to call them hot-exciton luminescence (HL) peaks, although actually the rest of the PSB except the part near the low-energy limit also originates from hot excitons, but with less energy.

The PSB₁ and PSB₂ are used to deduce the $S(E_k)$. To do this, we define the onset of the PSB₂ (E_{20} in Fig. 1) as its zero point of energy. The corresponding E_{10} of the PSB₁ is $E_{20} + E_{\text{LO}}$. With these definitions, the relative energy of the photon in each PSB, $E_{P1} - E_{10}$ for PSB₁ and $E_{P2} - E_{20}$ for PSB₂, equals the corresponding kinetic energy of excitons. In other words, the photon emitted in PSB₁ (PSB₂) with energy of E_{P1} (E_{P2}) originates from the first (second) order LO-phonon assisted recombination of excitons with kinetic energy E_k being equal to $E_{P1} - E_{10}$ ($E_{P2} - E_{20}$). From Eq. (1) and taking into account these relations, we have

$$S(E_k) = 2 \frac{I_2(E_{P2} - E_{20})}{I_1(E_{P1} - E_{10})}. \quad (3)$$

The deduced $S(E_k)$ is plotted in Fig. 2 as the solid curve. With increasing E_k , we see a rapid decrease of S . Decreasing E_{excess} , the measurable energy range becomes smaller and smaller since the PSB's are getting narrower. But the measurable parts overlap well with each other (not shown in Fig. 2). Another way to measure $S(E_k)$ is to use only the upper limit of the PSB's, the peaks HL₁ and HL₂, since the ratio between them reflects the S of excitons with corresponding value of E_k . Tuning E_{excess} thus varying the spectral position of the HL peak, we obtain $S(E_k)$, as

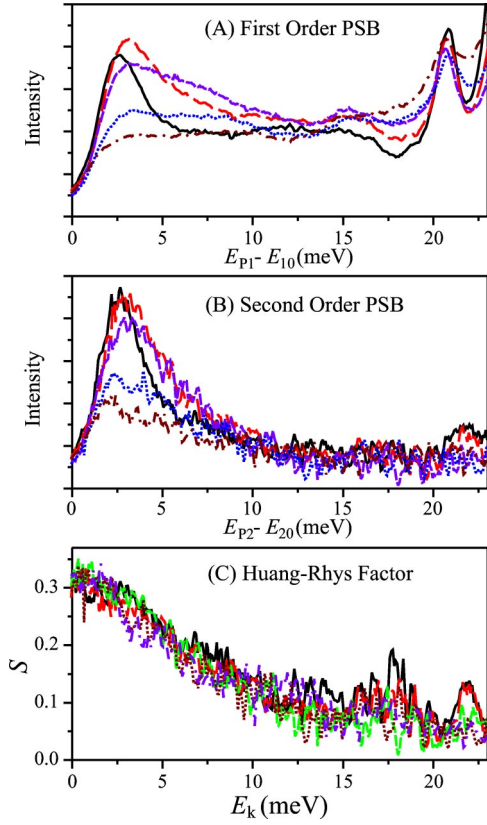


FIG. 3. (Color online) First order (A) and second order (B) PSB's measured at different temperatures and the deduced energy-dependent Huang-Rhys factors (C). The sample temperatures for these measurements are 8.2 K (solid line), 17.5 K (long-dashed line), 30.0 K (short-dashed line), 42.5 K (dotted line), and 52.3 K (dash-dotted line), respectively.

shown by the squares in Fig. 2. The result obtained with this method is well consistent with that by using the whole PSB's.

It is difficult to calculate from first principles the absolute values of S for free excitons in a particular structure. However, its *energy dependence* can be obtained quite straightforwardly from the model established by Permogorov.³⁷ We calculate the recombination rate of the first order LO-phonon-assisted luminescence,³⁸ and get the energy dependence of the S directly from this rate since the rate of the second order LO-phonon-assisted recombination is independent of E_k .³⁷ This yields

$$S(E_k) \propto \left| \frac{q(E_k - E_{LO})}{[1 + (a_0 q_c/2)^2]^{-2} - [1 + (a_0 q_v/2)^2]^{-2}} \right|^2. \quad (4)$$

Here a_0 is the exciton Bohr radius, q is the wave vector of the LO phonon, $q_{c,v} = q(\mu/m_{c,v})$, where $\mu = m_c m_v / (m_c + m_v)$ and the m_c , m_v are the effective masses of electron and hole, respectively. The calculated result is shown in Fig. 2 as the dashed line. For the excitons with $E_k > 3$ meV, the calculated curve is in good agreement with the experimental results except for an unknown scaling factor. But for cold excitons, the model predicts an infinite large value. We attribute the discrepancy between the theoretical and experi-

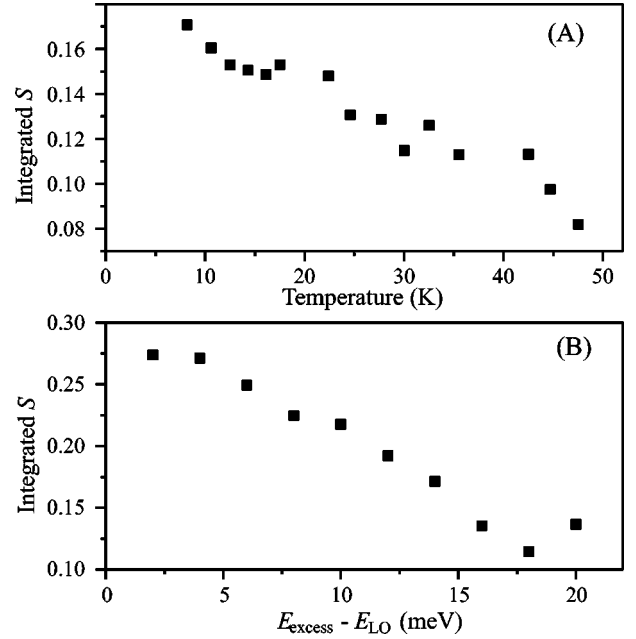


FIG. 4. Integrated Huang-Rhys factor measured by using the integrated intensity of PSB's to demonstrate the artefacts obtained in such experiments. (A) The alleged temperature effect. The excitation excess energy used is $E_{LO} + 14$ meV. (B) The alleged effect of excitation excess energy. The sample temperature is 7 K.

mental results for cold excitons to the persistence of static disorder in the sample, which can influence and localize the cold excitons. These effects may make this theoretical description invalid here by, e.g., relaxing the momentum conservation for cold excitons.

The $S(E_k)$ shown in Fig. 2 is important for PSB spectroscopy on hot excitons. Typically, the second order PSB is hard to be detected with a reasonable signal-to-noise ratio, especially in temporally or spatially resolved spectroscopy. Thus, the measured $S(E_k)$ provides a direct link between the measured first-order PSB to the real exciton distribution. More importantly, the additional energy dimension provides us deeper insight into the intrinsic properties of coupling between excitons and LO phonons. This is quite different from the typical experiments in which the energy-integrated S is measured, since the integration may average out the intrinsic features and lead to some artificial effects. As examples, we show below how the experimental conditions, i.e., temperature and E_{excess} , influence the measurement.

Figure 3 shows the measured first-order (A) and second-order (B) PSB spectra at different sample temperatures. In cw experiments, the steady distribution of excitons is determined by the dynamical balance between laser excitation, energy relaxation, and excitonic recombination. By increasing the temperature, the energy relaxation rate is reduced due to the enhanced acoustic-phonon absorption. This induces the change of the hot-exciton distribution toward the high-energy side, as clearly observed in Fig. 3(A,B). From these spectra, we deduce the $S(E_k)$ at different temperatures, as shown in Fig. 3(C). The result shows clearly that this factor is independent of sample temperature. Although this fact is quite obvious from the definition of the factor, measurements

exploiting the integrated intensity of PSB can lead to artificial temperature effects of integrated S . Figure 4(A) shows this effect quantitatively. By using the integrated intensity of PSB of the same sample the measured S decreases from 0.17 at low temperatures to 0.08 at 50 K. From Fig. 3, it is clear that this effect originates simply from a change of the hot-exciton distribution, thus a change of the weight for the integration. However, we note that the decrease of integrated S with increasing temperature was generally observed in this kind of experiments (see, e.g., Refs. 26,27), which is consistent with the artificial effect shown in Fig. 4(A).

Similar to the effect of sample temperature, the E_{excess} used in the experiment also influences the steady distribution of excitons, thus the measured integrated S . Figure 4(B) shows the integrated S measured with different E_{excess} . A pronounced decrease from 0.27 to 0.12 is observed when we change the initial value of E_k from 2 to 20 meV, being consistent with the strong energy dependence of the S as shown in Fig. 2. It is clear that such an artificial effect must be excluded. This can be achieved by measuring the energy-dependent S , instead of the integrated S .

In summary, quasiresonant excitation with low intensity at low temperature enables us to generate well-defined nonther-

mal distribution of hot excitons. This makes it possible to measure accurately the energy-dependent Huang-Rhys factor. We find that S decreases rapidly with increasing the kinetic energy of the exciton, which is consistent with the theoretical predictions. The factor describes the intrinsic properties of the coupling strength of the radiative transition to the LO-phonon polarization field and is independent of the sample temperature or excess energy of excitation. On the contrary, the integrated S typically measured in previous investigations shows strong effects on these experimental conditions since these conditions influence the exciton distribution. We confirm quantitatively that these effects are clearly artificial. We conclude that the energy-dependent Huang-Rhys factor, rather than the integrated one, should be measured in order to investigate the intrinsic properties of semiconductors and their heterostructures.

We acknowledge the growth of excellent samples by the group of M. Heuken (RWTH Aachen). This work was supported by the Deutsche Forschungsgemeinschaft (DFG) within Grant No. Ka 761/10-1 and within project A2 of the DFG-Center for Functional Nanostructures (CFN).

-
- ¹K. Huang and A. Rhys, Proc. R. Soc. London, Ser. A **204**, 406 (1950).
- ²X.B. Zhang, T. Taliercio, S. Kolliakos, and P. Lefebvre, J. Phys.: Condens. Matter **13**, 7053 (2001).
- ³W. Ungier and M. Suffczynski, Phys. Rev. B **18**, 4390 (1978).
- ⁴R. Heitz, H. Born, F. Guffarth, O. Stier, A. Schliwa, A. Hoffmann, and D. Bimberg, Phys. Rev. B **64**, 241305 (2001).
- ⁵D. Swiatla and W.M. Bartczak, Phys. Rev. B **43**, 6776 (1991).
- ⁶S. Nomura and T. Kobayashi, Phys. Rev. B **45**, 1305 (1992).
- ⁷I. Brener, M. Olszakier, E. Cohen, E. Ehrenfreund, A. Ron, and L. Pfeiffer, Phys. Rev. B **46**, 7927 (1992).
- ⁸J.C. Marini, B. Stebe, and E. Kartheuser, Phys. Rev. B **50**, 14302 (1994).
- ⁹M.R. Silvestri and J. Schroeder, Phys. Rev. B **50**, 15108 (1994).
- ¹⁰T. Telahun, U. Scherz, P. Thurian, R. Heitz, A. Hoffmann, and I. Broser, Phys. Rev. B **53**, 1274 (1996).
- ¹¹T. Takagahara and K. Takeda, Phys. Rev. B **53**, 4205 (1996).
- ¹²J.C.M. Henning, F.P.J. de Groote, W.C. van der Vleuten, and J.H. Wolter, Phys. Rev. B **53**, 15802 (1996).
- ¹³T.D. Krauss and F.W. Wise, Phys. Rev. B **55**, 9860 (1997).
- ¹⁴A.V. Baranov, S. Yamauchi, and Y. Masumoto, Phys. Rev. B **56**, 10332 (1997).
- ¹⁵V. Türec, S. Rodt, O. Stier, R. Heitz, R. Engelhardt, U.W. Pohl, D. Bimberg, and R. Steingrüber, Phys. Rev. B **61**, 9944 (2000).
- ¹⁶T. Makino, K. Tamura, C.H. Chia, Y. Segawa, M. Kawasaki, A. Ohtomo, and H. Koinuma, Phys. Rev. B **66**, 233305 (2002).
- ¹⁷M. Smith, J.Y. Lin, H.X. Jiang, A. Khan, Q. Chen, A. Salvador, A. Botchkarev, W. Kim, and H. Morkoç, Appl. Phys. Lett. **70**, 2882 (1997).
- ¹⁸R. Heitz, H. Born, A. Hoffmann, D. Bimberg, I. Mukhametzhanov, and A. Madhukar, Appl. Phys. Lett. **77**, 3746 (2000).
- ¹⁹V.V. Fedorov, S.B. Mirov, M. Ashenafi, and L. Xie, Appl. Phys. Lett. **79**, 2318 (2001).
- ²⁰M. Soltani, M. Certier, R. Evrard, and E. Kartheuser, J. Appl. Phys. **78**, 5626 (1995).
- ²¹M. Germain, E. Kartheuser, A.L. Gurskii, E.V. Lutsenko, I.P. Marko, V.N. Pavlovskii, G.P. Yablonskii, K. Heime, M. Heuken, and B. Schineller, J. Appl. Phys. **91**, 9827 (2002).
- ²²U. Woggon, E. Lüthgens, H. Wenisch, and D. Hommel, Phys. Rev. B **63**, 073205 (2001).
- ²³D. Kovalev, B. Averboukh, D. Volm, B.K. Meyer, H. Amano, and I. Akasaki, Phys. Rev. B **54**, 2518 (1996).
- ²⁴E. Oh, S.K. Lee, S.S. Park, K.Y. Lee, I.J. Song, and J.Y. Han, Appl. Phys. Lett. **78**, 273 (2001).
- ²⁵M. Leroux, N. Grandjean, B. Beaumont, G. Nataf, F. Massies, and P. Gibart, J. Appl. Phys. **86**, 3721 (1999).
- ²⁶M. Wojdak, A. Wyszomolek, K. Pakula, and J.M. Baranowski, Phys. Status Solidi B **216**, 95 (1999).
- ²⁷W. Liu, M.F. Li, S.J. Xu, K. Uchida, and K. Matsumoto, Semicond. Sci. Technol. **13**, 769 (1998).
- ²⁸D.C. Reynolds, D.C. Look, D.N. Talwar, G.L. McCoy, and K.R. Evans, Phys. Rev. B **51**, 2572 (1995).
- ²⁹S.S. Prabhu, A.S. Vengurlekar, and J. Shah, Phys. Rev. B **53**, 10465 (1996).
- ³⁰C.D. Poweleit, L.M. Smith, and B.T. Jonker, Phys. Rev. B **55**, 5062 (1997).
- ³¹S.J. Xu, W. Liu, and M.F. Li, Appl. Phys. Lett. **81**, 2959 (2002).
- ³²S. Kalliakos, X.B. Zhang, T. Taliercio, P. Lefebvre, B. Gil, N. Grandjean, B. Damilano, and J. Massies, Appl. Phys. Lett. **80**, 428 (2002).
- ³³M. Umlauff, J. Hoffmann, H. Kalt, W. Langbein, J.M. Hvam, M. Scholl, J. Söllner, M. Heuken, B. Jobst, and D. Hommel, Phys. Rev. B **57**, 1390 (1998).

- ³⁴H. Zhao, S. Moehl, and H. Kalt, Phys. Rev. Lett. **89**, 097401 (2002).
- ³⁵H. Zhao, S. Moehl, S. Wachter, and H. Kalt, Appl. Phys. Lett. **80**, 1391 (2002).
- ³⁶H. Zhao, B. Dal Don, S. Moehl, H. Kalt, K. Ohkawa, and D. Hommel, Phys. Rev. B **67**, 035306 (2003).
- ³⁷S. Permogorov, in *Excitons*, edited by E.I. Rashba and M.D. Sturge (North-Holland, Netherlands, 1982), Chap. 5.
- ³⁸H. Zhao, S. Moehl, and H. Kalt, Appl. Phys. Lett. **81**, 2794 (2002).